



IJRASET

International Journal For Research in
Applied Science and Engineering Technology



INTERNATIONAL JOURNAL FOR RESEARCH

IN APPLIED SCIENCE & ENGINEERING TECHNOLOGY

Volume: 9 Issue: VIII Month of publication: August 2021

DOI: <https://doi.org/10.22214/ijraset.2021.37834>

www.ijraset.com

Call:  08813907089

E-mail ID: ijraset@gmail.com

2 Way Fluid-Structure Interaction Study of a Wing Structure

Prathik S Jain¹, Varun C², Shivani Shankar³, Kshiti P Gowda⁴, Shrey Kumar Jain⁵

¹Asst. Professor, Department of Aeronautical Engineering, Dayananda Sagar College of Engineering, Kumaraswamy Layout, Bangalore -560078, Karnataka, India

^{2, 3, 4, 5}Students, Department of Aeronautical Engineering, Dayananda Sagar College of Engineering, Kumaraswamy Layout, Bangalore -560078, Karnataka, India

Abstract: In this paper a scaled down model of a wing of rectangular planform is designed and the static analysis on the wing is carried out to determine the aerodynamics forces, stresses acting on it and the frequency of various modes. The iteration for the analysis is carried out for three materials namely, Aluminium 7075 T-6, Glass Fibre Reinforced Polymer and Aluminium Metal Matrix Composite. The analysis in the coupled mode is conducted and compared with the results obtained from that of static analysis to observe the changes in the flow pattern and how the structure behaves when the wing is considered to be flexible. In the coupled mode analysis 2 Way Fluid Structure Interaction analysis is carried out. The material properties and the results obtained from the analysis is compared to select the best out of the three materials. The change in the aerodynamic properties of the wing when it is considered to be flexible is also highlighted by a method of comparison. From the results obtained, it is observed that Aluminium Metal Matrix Composite has the least deformation for the same loading and can withstand higher stress. Hence, Aluminium Metal Matrix Composite exhibits better characteristics in comparison with Glass Fibre Reinforced Polymer and Aluminium 7075 T-6. Additionally, it is noticed that the aerodynamic properties of the wing is reduced when it is considered as a flexible structure. This can be highlighted by the 5.42% decrease in the L/D ratio between the CFD analysis and the 2 Way FSI analysis results.

Keywords: Fluid Structure Interaction; Flexible Wing; CFD; Coupled Mode Analysis;

I. INTRODUCTION

Fluid-Structure Interaction is the multi-physics coupling between the laws governing structural mechanics and that of fluid dynamics. When a body or structure is present in the flow there are stresses and strains which are exerted by the fluid on the solid body, these forces exerted lead to the deformation of the structure. The deformation which is caused in the solid because of the fluid in turn produces an effect on the flow and the pressure fields of the fluid, the deformation caused produces a change in the properties of the flow and thus Fluid-Structure Interaction is the coupling between structural mechanics and fluid dynamics. Fluid-Structure Interactions play a very vital role and thus have to be taken into account for the design of many engineering systems such as aircrafts, engines and spacecrafts. In the structures which consist of materials susceptible to fatigue, these oscillatory interactions can be extremely detrimental. Fatigue is the cyclic loading which causes the development of cyclic stresses and strains in the material, under this loading at a critical loading the material fails. An aircraft wing at the time of flight is subjected to various loads which result in the deformation of the wing and oscillation in the wing which poses a challenge for the design of the structure and for its safety, the loads which are acting on the wing can lead to the formation of a crack at the region of high stress concentration which propagates till it reaches a maximum value beyond which the aircraft wing structure will fail due to fatigue. Thus aircraft wings are structures which are highly susceptible of fatigue and so consideration of FSI for the aircraft wing structure is of great importance. Due to various undesired phenomenon such as fluttering, buffeting in aircrafts the interaction between fluid and flexible aircraft wing have extreme importance. The fluid-structure interaction on an aircraft wing. In some of the previous work carried out the desired wing was modelled in CATIA V5R21. Then, the wing was analyzed for the aerodynamic performance under the given flight conditions. The pressure distribution resulted from the flow analysis is then applied as a structural load over the wing. The computations were performed for AGARD 445.6 wing by considering the transonic flow at subsonic mach numbers [1]. Dynamic fluid structure interaction analysis of propeller aircraft wing was carried out, dynamic fluid structure interaction analysis was carried out by combining CFD and CSD solver to predict effect of fluid forces on wing structural behaviour and of deformation on aerodynamic efficiency, wing was designed using airfoil NACA2412 the model of wing is then imported to ANSYS software where the fluid domain around the wing is generated in ANSYS design modeler to simulate flow effects. Solid aircraft wing is then subtracted from fluid domain by preserving both fluid as well as structural domain.

Research results revealed that there is 5.64% decrease in Lift-to-Drag ratio by considering wing as flexible structure [2]. In the previous work [3] examined the fluid structure interaction for light aircraft wing structure (SAFAT 03 wing structure) that was modelled using CATIA software. Galerkin energy method was applied to calculate the flutter and divergence speed and a MATLAB code was used in order to calculate the flutter speed. The fluid structure interaction approach has been used in ANSYS and the problem is setup in ANSYS environment and tested using a typical wing configuration. The aeroelastic effects of a very flexible transonic wing was analyzed in some previous research work [4] using fluid static interaction a computational aeroelastic study of a three-dimensional transonic wing model was carried out to achieve this a new partitioned FSI solver have been compiled, starting from Open-source software. The final results showed large displacements, leading to a clear motion of the shocks waves along the wing chord and great variation in the flight performances. he fluid-structure interaction behaviour of a cropped delta wing was analyzed using a CFD based aeroelastic solver in time domain. An N-S based finite volume solver was coupled with a finite element based linear and nonlinear structural solvers to study the nonlinear aeroelastic characteristics of the delta wing over a range of dynamic pressures. The amplitude and frequency obtained from the present coupled solver at various dynamic pressures were compared with the available experimental and computational results [5]. The vibratory reliability analysis of an aircraft wing was carried out using fluid structure interaction, a numerical vibratory study was conducted on a three-dimensional aircraft’s wing subjected to aerodynamic loads. Finite volume method (FVM) was used for the discretization of the fluid problem, and finite element method (FEM) was used for the structure’s approximation. The set of reliability tools is based on FORM and SORM methods. The results obtained showed the potentialities of the procedure methodology for use in complex coupled fluid–structure systems especially for aeroelastic ones [6].

The Fluid-Structure Analysis conducted would provide a deeper insight about the interaction between the solid structure and fluid when the structure is considered flexible and the results of the FSI Analysis is compared with that of CFD analysis where the aircraft wing is considered as a rigid structure and the variation in the results are observed and the results are compared.

II. METHODOLOGY

A. Selection of Airfoil

Five airfoils were selected based on the required criteria namely Eppler 421, Eppler 423, FX 74, NACA 2415 and Selig 1223. XFLR5 was used to plot the airfoil polars at a Reynolds Number of 250000 which corresponds to a velocity of 15m/s. The graphs between C_l vs Alpha, C_m vs Alpha, C_l vs C_d , C_d vs Alpha and C_l/C_d vs Alpha are plotted and is shown in Fig 1-5.

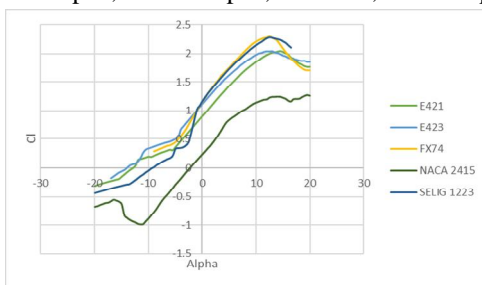


Fig.1 : C_l vs Alpha

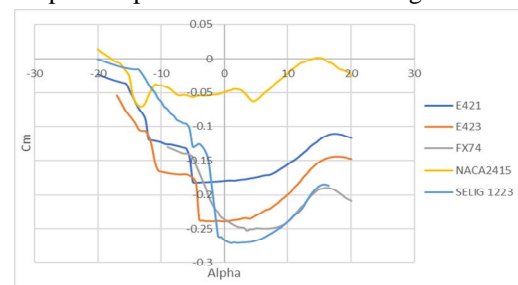


Fig. 2: C_m vs Alpha

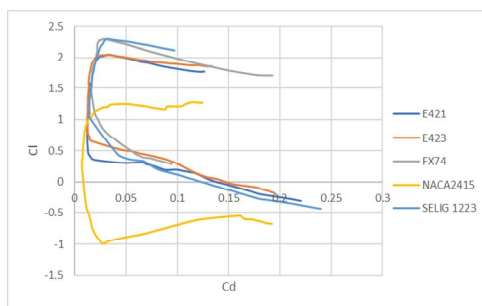


Fig. 3: C_l vs C_d

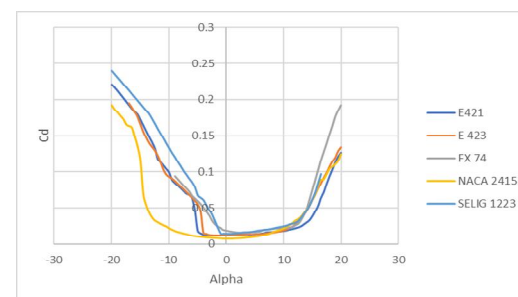


Fig. 4: C_d vs Alpha

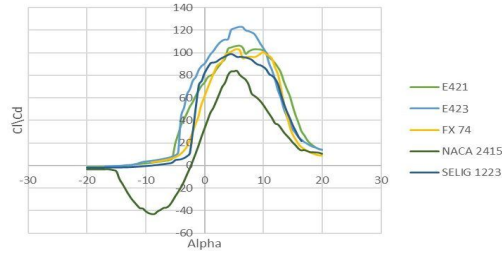


Fig. 5: C_l/C_d Vs Alpha

Eppler 423 and Selig 1223 were shortlisted after comparing the five airfoils since they had the best aerodynamic characteristics and to select between the airfoils Eppler 423 and Selig 1223 a Pugh matrix is employed where fabrication, C_{lmax} , C_l/C_d are the parameters chosen for the selection. The airfoils are rated on a scale of 1 to 5 based on their compatibility to the requirements, where 5 indicates the highest rating and 1 indicates the lowest rating respectively. Fabrication and C_l/C_d are considered to be the most important parameters hence they are given a rating of 5 followed by C_{lmax} which is rated at 4. Taking the ratings into consideration, Eppler 423 and Selig 1223 are rated after carefully evaluating the polars and their ease of fabrication. It is also noticed that it is easier to fabricate Eppler 423 due to its relatively thick trailing edge when compared to Selig 1223. The Pugh matrix is shown in the Table 1 :

TABLE 1
Airfoil Selection Pugh Matrix

Parameters	Weight	Airfoil	
		Eppler 423	Selig 1223
Fabrication	5	5	4
C_{lmax}	4	3	4
C_l/C_d	5	5	4
Total	-	62	56

Eppler 423 is chosen among the five airfoils considered since it has a higher total score of 62 compared to that of Selig 1223 which has a total score of 56.

The aerodynamic characteristics of E423 obtained from XFLR5 airfoil polars is specified in Table 2 :

Table 2
EPPLER 423 Characteristics

C_{lmax}	C_{lmin}	C_{l0}	C_{dmin}	Stall Angle
2.0035	0.0419	1.1905	0.0192	12.25°

B. Material Selection

Three different materials from the categories of an alloy, composite and polymer are chosen so as to compare the behaviour of different material under similar loadings. The materials selected are given in table 3:

Table 3
Material Properties

Material	Young's Modulus (GPa)	Density (kg/m ³)	Yield Strength (MPa)	Ultimate strength (MPa)
Aluminium 7075-T6	70	2810	503	572
Glass Fibre Reinforced Polymer	30	2630	1800	2050
Aluminium Metal Matrix Composite	250	3400	1200	1230

C. Wing Configuration

The airfoil coordinates are imported onto CATIA V5. The wing is of rectangular plan form and has 7 ribs, 10 stringers of circular cross section and 2 spars of I cross-section. The wing is of a span of 1.52 m, the wing span is the distance measured from one wingtip to the other wingtip. The chord is 0.254m, the chord of the wing is the distance measured from the leading edge to the trailing edge of the wing. The aspect ratio is 6, the aspect ratio is the ratio of the span of the wing to its mean chord. The dimensions of the wing are specified in Table 4 below:

TABLE 4
WING DIMENSIONS

Planform	Span	Chord	Aspect Ratio
Rectangular	1.52m	0.254m	6

The rendered wing structure images are shown in the Fig. 6. Fig. 6(a) shows the image of the wing with the skin and Fig. 6(b) shows the image of the wing without the skin.

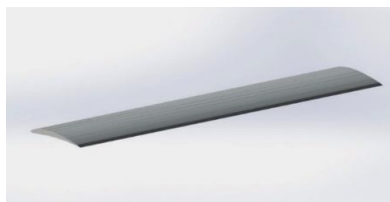


Fig. 6(a) : Wing with Skin

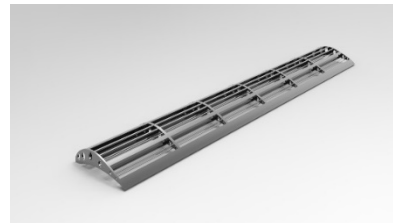


Fig. 6(b) : Wing without Skin

D. Loading

The average weight of a conventional two seater aircraft is taken into consideration to apply the load. In order to reduce the computation time the wing span is scaled down to a ratio of 10:1 therefore the weight of the aircraft is also taken in the same ratio. Wings are the important structures in an aircraft and carry 80% of the total load of the aircraft [7]. The following calculations are carried out to determine the loading:

Average weight of a two seater aircraft = 937 kg

Scaled down weight, w = 93.7 kg

Actual force acting on aircraft = w x g
= 937 N

Load acting on the wings = 80% of the total load
= 749.6 N

Therefore, a uniformly distributed load of 749.6 N is applied on the spars of the aircraft. This force is defined as a vector which is directed in the downward direction.

III. CFD ANALYSIS

A. Grid Independence Study

The study is conducted by varying the element size. The element size is first considered as 0.03 and the number of elements and number of nodes for the element size is noted and the lift obtained is 57.27 N. The size of the element is decreased to 0.02 and the number of elements and number of nodes corresponding to this element size is noted and the lift obtained is 57.5 N. The size of the element is further decreased to 0.01 and the number of elements and number of nodes corresponding to this size is noted and the lift obtained is 55.6 N. The theoretical lift is calculated using :

$$L = \frac{1}{2} C_L \rho v^2 S \tag{1}$$

Where, ρ : Density (kg/m³) = 1.225 kg/m³

L : Lift (N)

C_L : Lift Coefficient = 1.1 (at 0° Angle of Attack)

S : Wing Reference Area (m²) = 0.386 m²

v : Velocity (m/s) = 15 m/s

On calculation, the theoretical lift is found to be 58.5 N. Since the lift obtained using element size 0.02 is 57.5 N which is the closest to the theoretical value, the element size of 0.02 is selected. Table 6 indicates the values of number of elements, number of nodes and the lift value for the element size 0.03, 0.02 and 0.01 respectively

Table 5
GRID Independence Study

Element Size	0.03	0.02	0.01
Number of Elements	581694	851661	1899629
Number of Nodes	113250	160226	338613
Lift (N)	57.27	57.5	55.6

B. Boundary Conditions

The boundary conditions set for the fluent module in order to carry out CFD Analysis is given in table 6 below:

Table 6
Boundary Conditions

Viscous Model	Spalart Allmaras
Materials	Air
Boundary Conditions	Velocity Inlet : 15m/s Pressure outlet : 0 Pa
Reference Value	Compute from : Inlet Select body : Solid
Monitors	Lift and Drag monitors On
Initialization	Hybrid Initialization
Calculation	500 iterations

IV.2 WAY FSI ANALYSIS

In two way FSI the transient static structural module and fluent module are coupled with the help of system coupling and the data transfer takes place from transient module to fluent module and back from fluent module to transient module in a cyclic manner this analysis is carried out till the desired end time step is reached. The solution algorithm used for One Way Fluid Structure Interaction Analysis is shown in Fig. 7.

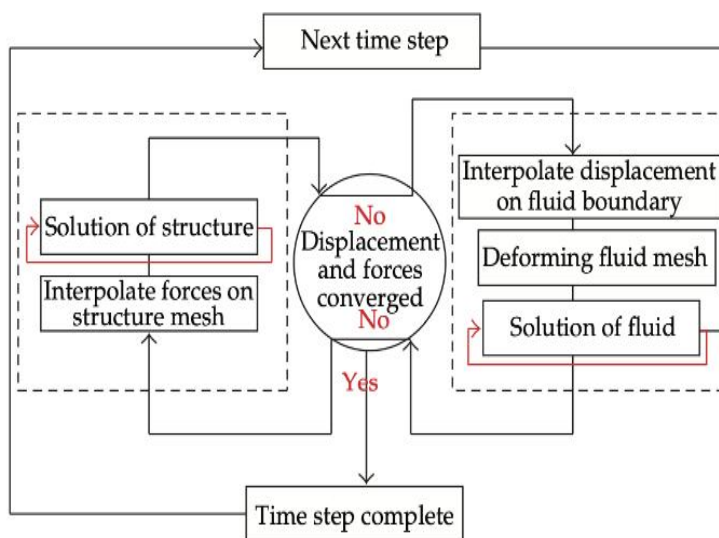


Fig. 7: 2 Way FSI Algorithm

A. Boundary Conditions

The boundary conditions specified for the transient static structural module is as given in the table 7 below:

TABLE 7
Transient Module Boundary Conditions

Fixed Support	Geometry : 1 face (Wing considered as cantilever beam)
Loading	749.6 N uniformly distributed and acting downwards direction
Fluid Solid Interface	Geometry : 4 faces
Analysis Settings	Number of Steps : 1 Current Step Number : 1 Step End Time : 20 s Auto Time Stepping : Off Define By : Time Time Step : 1 s Time Integration : On

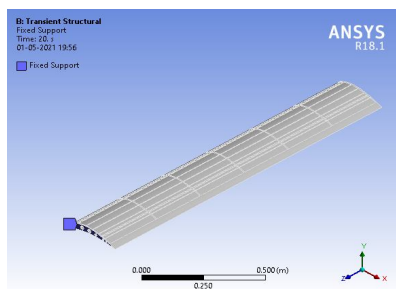


Fig. 8 : Fixed Support

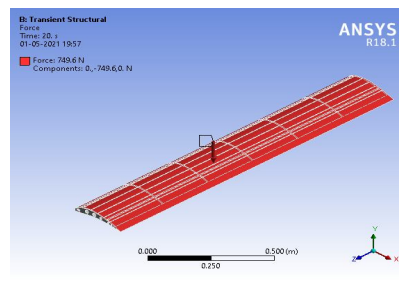


Fig.9: Load acting on Wing

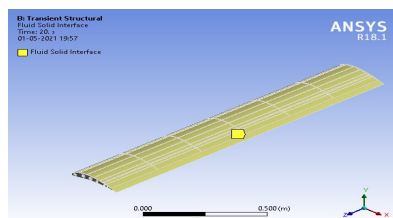


Fig. 10 : Fluid Solid Interface

B. Boundary Conditions for Fluent Module

The set up for the fluent module is given in table 8 below:

TABLE 8
Boundary Conditions

Viscous Model	Spalart Allmaras
Materials	Air
Boundary Conditions	Velocity Inlet : 15m/s Pressure outlet : 0 Pa
Dynamic Mesh	Zone : Wing Type : System Coupling
Initialization	Hybrid Initialization
Calculation	Time Step Size : 0.001 s Number of Time Steps : 20 Max Iterations / Time Step : 10 Reporting Interval : 1 Profile Update Interval : 1

C. System Coupling

1) *Data Transfer:* The wing from the Fluent Module and the Fluid Solid Interface from the Transient Structural Module are selected together to create the data transfer between the two modules. Fig. 11 illustrates the data transfer established between the two modules. Data Transfer 1 indicates a transfer in which the source is the Fluent Module and the target is the Transient Structural Module. Fig. 12 depicts the same. Data Transfer 2 indicates a transfer in which the source is the Transient Structural Module and the target is the Fluent Module. Fig. 13 depicts the working of Data Transfer 2.

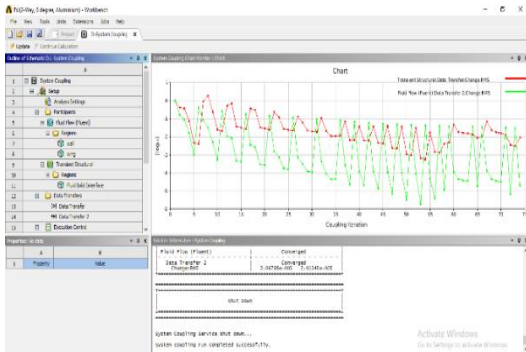


Fig. 11 : System Coupling Data Transfer

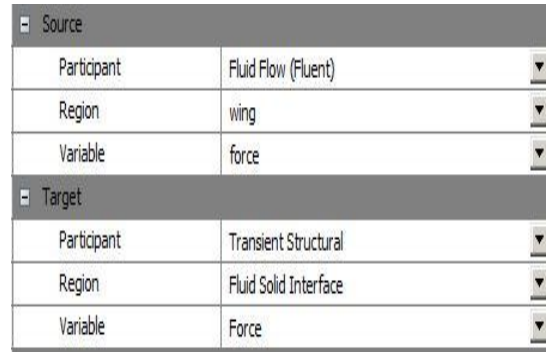


Fig. 12 : System Coupling Data Transfer

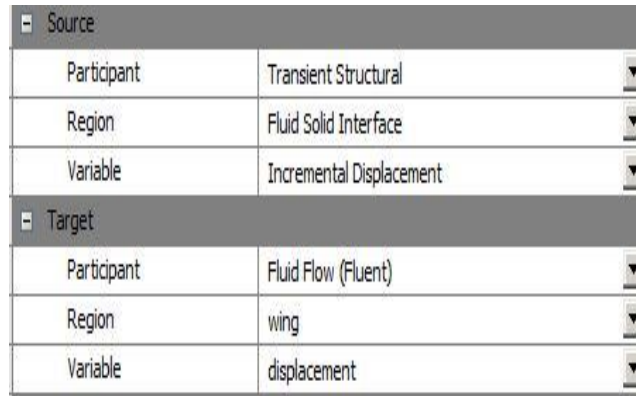


Fig. 13 : System Coupling Data Transfer

2) *Analysis Setting:* The analysis setting for the system coupling is as shown in table 9 :

Table 9
Analysis Settings

Coupling Initialization	Program Controlled
Duration Defined By	End Time
End Time	2 s
Step Size	0.1 s
Minimum Iterations	1
Maximum Iterations	5

V. RESULTS

A. CFD Results

The calculation was run for 500 iterations and the solution converged at 311th iteration. Lift and Drag monitors were obtained for 0° and 20° Angle of Attack given in Table 10.

TABLE 10
Lift And Drag Monitors

Angle of Attack	Drag (N)	Lift (N)	Lift/Drag
0°	1.6968	57.506	33.89085
2°	1.8443	68.219	36.9891
4°	2.1903	77.575	35.41752
6°	2.6503	86.269	32.55065
8°	3.4663	92.16	26.58743
10°	4.2136	97.832	23.21815
12°	5.5651	99.398	17.86095
12.25°	5.8682	99.432	16.94421
12.5°	5.9424	99.07	16.67172
14°	7.72793	97.635	12.63404
15°	8.2639	97.24	11.76684
15.25°	8.2271	97.006	11.79103
15.5°	8.2689	97.995	11.85103
15.75°	8.6901	94.992	10.93106
16°	9.4205	93.125	9.885356
18°	11.189	93.415	8.348825
20°	14.71	83.277	5.661251

The 3-dimensional aerodynamic characteristics(lift, drag and lift to drag ratio) for various angles of attack are obtained from ANSYS R18.1 and the resultant graphs are plotted which are shown from Fig. 14 to Fig. 16.

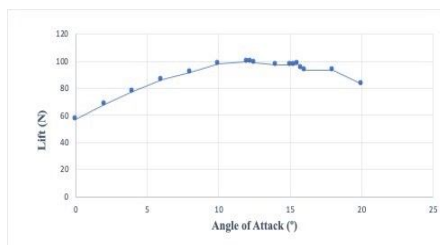


Fig. 14: Lift Vs Angle of Attack

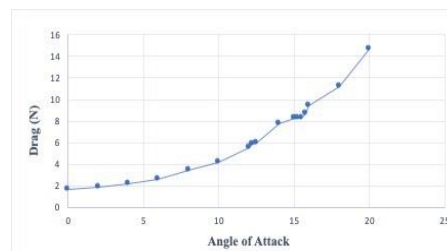


Fig. 15: Drag vs Angle of Attack

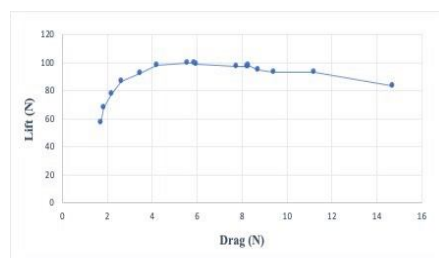


Fig. 16: Lift vs Drag

1) *Velocity Contours*: From the velocity contour, we can observe that the velocity is minimum at the leading edge of the wing which is represented by the blue contour. The maximum and minimum values of velocity obtained from the fluent analysis for an AOA of 0° and 12.25° is given in Table 11:

Table 11
Velocity Plot

	Velocity (m/s)	
Angle of Attack 0°	Minimum	0.000e+000
	Maximum	2.224e+001
Angle of Attack 12.25°	Minimum	0.000e+000
	Maximum	2.791e+001

Fig. 17 shows the velocity contours obtained for a velocity of 15 m/s at 0° and 12.25°

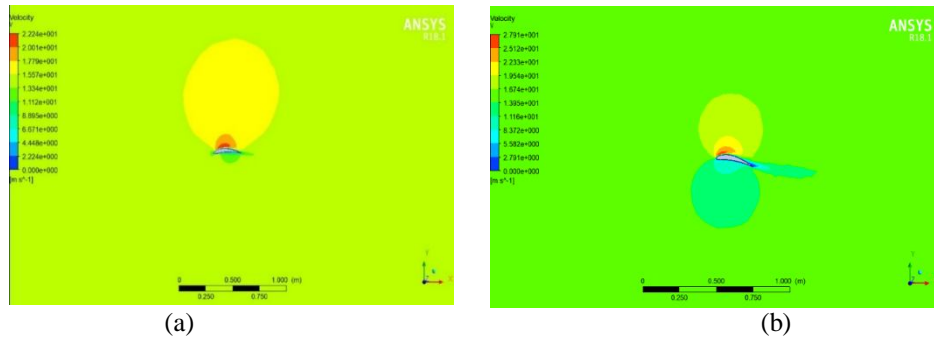


Fig. 17: (a) Velocity Contours for 0° AOA (b) Velocity Contours for 12.25° AOA

2) *Pressure Contours*: From the pressure contours it is observed that the pressure is maximum at the leading edge which is indicated by the red contour. This pressure is called stagnation pressure and the velocity is minimum at this point. The maximum and minimum values of pressure for 0° and 12.25° AOA obtained from the fluent analysis is given in Table 12 :

Table 12
Pressure Plot

	Pressure (Pa)	
Angle of Attack 0°	Minimum	-1.960e+002
	Maximum	1.2251e+002
Angle of Attack 12.25°	Minimum	-4.237e+002
	Maximum	1.379e+002

Fig. 18 shows the pressure contours obtained for a velocity of 15 m/s at 0° and 12.25°

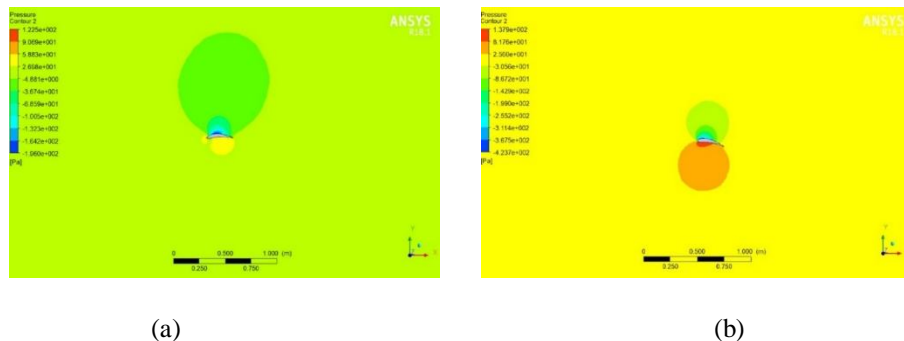


Fig. 18: (a) Pressure Contours for 0° AOA (b) Pressure Contours for 12.25° AOA

B. 2 Way FSI Results

1) **Fluid Flow Analysis:** The results obtained from 2 way fluid-structure interaction for AMC is discussed below, the mapping which indicates the data transfer between transient structural and fluid flow fluent module is carried out successfully as shown in Fig. 19.

MAPPING SUMMARY		
Data Transfer Diagnostic	Source Side	Target Side
Data Transfer		
Percent Nodes Mapped	99	99
Percent Area Mapped	98	100
Data Transfer 2		
Percent Nodes Mapped	N/A	100

Fig. 19 : Mapping Summary

The pressure contour indicates the distribution of pressure over the surface of the wing. From the pressure contours it is observed that the pressure is maximum at the leading edge which is indicated by the red contour. This pressure is called stagnation pressure and the velocity is minimum at this point. In addition, it can be observed the pressure on the surface of the wing is increased because of the effect of structural deformation.

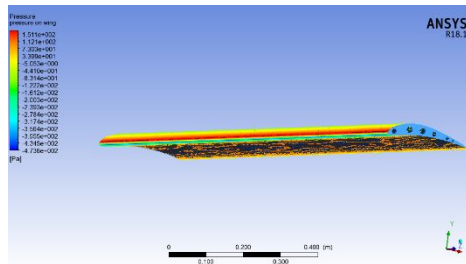


Fig. 20 : Pressure Contour

A plane is created at the mid-section and the tip of the wing to see the pressure distribution at these sections. It can be observed from the contours that the deformation in the structure affects the pressure fields in the fluid domain as shown in Fig. 21 and Fig. 22 and the velocity plot is shown in Fig. 23.

Similar procedure is carried out for Aluminium 7075 T-6 alloy and Glass Fibre Reinforced Polymer and the pressure plots and velocity plots for the materials was obtained.

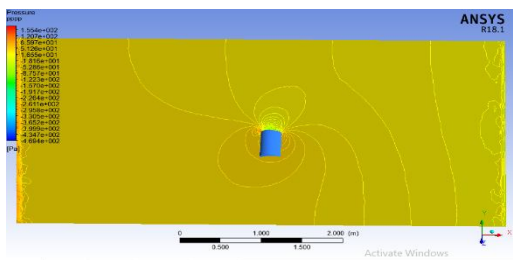


Fig. 21 : Pressure Contour 5 (AMC)

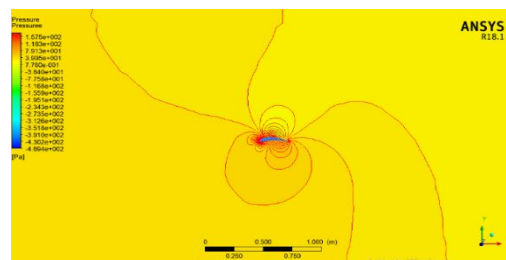


Fig. 22 : Pressure Contour 6 (AMC)

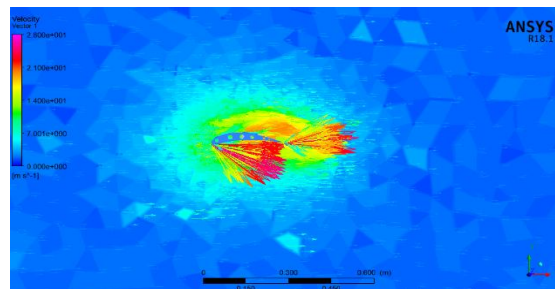


Fig. 23 : Velocity Plot (AMC)

2) *Transient Structural Analysis*: The deformation vs time, stress vs time and strain vs time data shown in Fig. 24-26 was extracted from the transient structural module of the fluid structure interaction analysis for all the three materials namely Aluminium 7075 T-6, GFRP, AMC. The data was extracted for a duration of 2 seconds with a time step of 0.1 second. It can be observed from the graph that AMC deforms the least over time while GFRP deforms the most.

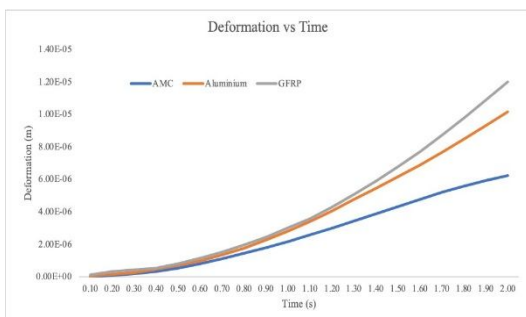


Fig. 24 : Deformation Vs Time

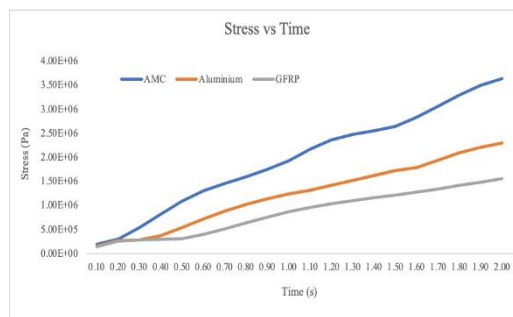


Fig. 25 : Stress Vs Time

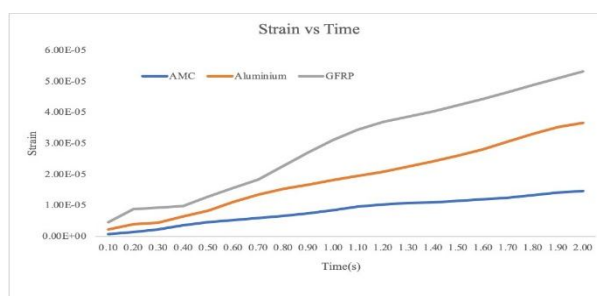


Fig. 26: Strain Vs Time

VI. COMPARISON OF RESULTS

In order to verify the theoretical lift values with the analytical lift values obtained from the CFD analysis, the results are compared. The values of lift – coefficient for various angles of attack is obtained from the XFLR5 analysis carried out on Eppler 423. A percentage change of 5% to 10% between the results is considered acceptable since this variation depends on the meshing as well as the boundary conditions used.

The theoretical and analytical lift values obtained for different AOA is given in table 13 :

TABLE 13
Comparison Of Theoretical And Analytical Lift Values

Angle Of Attack (°)	Lift (N) (Theoretical)	Lift (N) (Analytical)	Percentage Change (%)
0	58.5151875	57.506	1.724
2	69.154	68.219	1.352
4	79.7934	77.575	2.780
6	87.113	86.269	1.358
8	95.7521	92.16	3.7514
10	101.0716	97.832	3.2053
12	106.3912	99.398	6.5731
12.25	108.5190	99.432	8.3737
12.5	107.9871	99.07	8.2575
14	106.9232	97.635	8.686
15	104.2634	97.24	6.7362
15.25	103.7314	97.006	6.48353
15.5	103.1995	97.995	5.0431
16	101.0716	93.125	7.8624
18	95.752	93.425	2.3404
20	94.6882	83.77	12.05

The values of theoretical and analytical lift are plotted against the Angle of Attack as shown in Fig. 27.

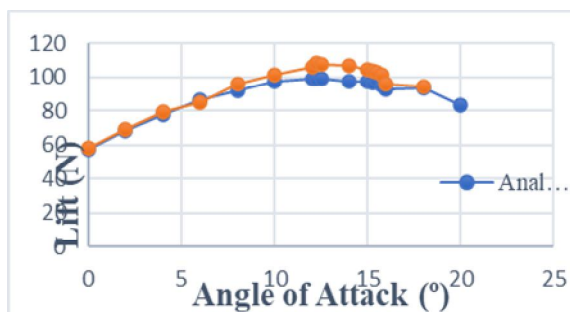


Fig. 27 : Comparison of Theoretical and Analytical Lift Values

The lift, drag and the L/D values obtained by CFD and 2 Way FSI analysis are compared and plotted to observe the variation. Table 14 shows the comparison of the analytical lift values with the values obtained from the 2 Way FSI analysis.

Table 14
Comparison of CFD and 2 Way FSI Lift Values

Angle of Attack (°)	Lift (N)	Lift (N) (2 Way FSI)
0	58.5151	41.19
2	69.1543	48.679
4	79.7934	56.030
8	95.7521	67.342
10	101.0716	70.972
12.25	108.5190	76.321
14	106.9232	75.124

Table 15 shows the comparison of the analytical drag values with the values obtained from the 2 Way FSI analysis.

Table 15
Comparison of CFD and 2 Way FSI Drag Values

Angle of Attack (°)	Drag (N)	Drag (N) (2 Way FSI)
0	6.5909	4.8953
2	0.6702	0.4978
4	0.7298	0.5424
8	0.8378	0.6230
10	1.0112	0.7550
12.25	1.4894	1.1086
14	2.4438	1.808

From the lift and drag values obtained from the 2 Way FSI analysis, the L/D ratio is calculated. An average of the percentage change is calculated and it is found to be 5.42%. These values are tabulated along the percentage change as shown in Table 16.

TABLE 16
Comparison of CFD and 2 way FSI L/D Values

Angle of Attack (°)	L/D	L/D (2 Way FSI)	Percentage Change (%)
0	8.8781	8.414	5.225
2	103.1746	97.783	5.225
4	109.3294	103.284	5.5293
8	114.2857	108.091	5.4195
10	99.9474	93.9909	5.9595
12.25	72.8571	68.843	5.5085
14	43.7527	41.530	5.079
Average			5.42

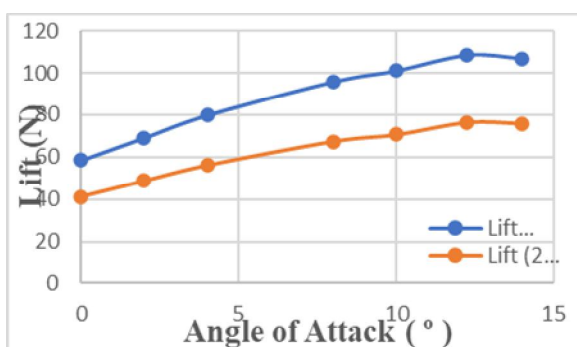


Fig. 28 : Comparison of CFD and 2 Way FSI Lift Values

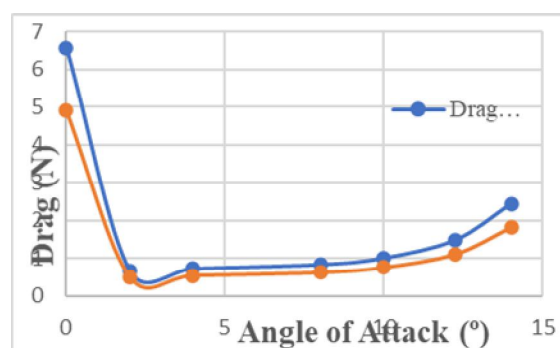


Fig. 29 : Comparison of CFD and 2 Way FSI Drag Values

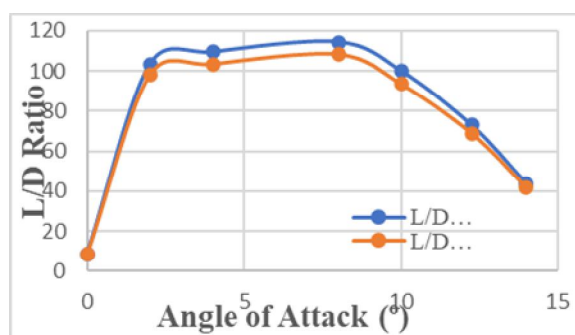


Fig. 30 : Comparison of CFD and 2 Way FSI L/D Values

VII. CONCLUSION

The aerodynamic and structural behaviour of the wing varies greatly when a coupled analysis is carried out on it. This in turn is capable of mimicking the actual phenomenon that the aircraft would experience in real time. Fluid Structure Interaction, being a fairly new topic of research has gained a lot of traction due to its increasing application in understand this particular behaviour of the aircraft. The interaction between fluid and flexible structure plays a vital role in many engineering applications such as flutter in aircraft wings, fluid excited vibrations to name a few. Eppler 423 was chosen as the airfoil and the wing was designed on CATIA V5. Three materials were chosen for the analysis to compare the behaviour of different materials namely Aluminium 7075 T-6, GFRP and AMC. By carrying out CFD analysis it was found that at 12.25° stall occurs and thus it is the stall angle. The velocity and pressure contours are obtained for two angles of attack which are 0° and 12.25°. The maximum velocity for 0° is 2.224e+001 m/s and that for 12.25° is 2.791e+001 m/s. Two way FSI analysis was carried out for the three materials by coupling the transient structural module and fluent module.



The pressure and velocity contours are obtained from the fluent module and the deformation, Von-Mises stress and strain values are obtained from transient structural module, on comparing the values of deformation for the three materials it is observed that AMC has the least deformation followed by Aluminium 7075T-6 alloy and GFRP has the highest deformation, consequently AMC has the highest equivalent Von-Mises Stress value indicating that it can resist higher values of stress. On close observation of the results obtained from the Fluent side of the 2 Way FSI analysis it can be seen that the lift values drastically reduces when the wing is considered to be flexible for instance at 0° the value of lift decreases from 58.51 N to 41.19 N. This reduction in lift values occurs due to the change in the flow properties caused by the structural deformations of the structure. The L/D values from the 2 Way FSI analysis shows an average decrease of 5.42% in comparison with the CFD results.

REFERENCES

- [1] T. Sai Kiran Goud, Sai Kumar A, Dr. S Srinivasa Prasad, (2014) "Analysis of Fluid-Structure Interaction on an Aircraft Wing". International Journal of Engineering and Innovative Technology, Volume 3, Issue 9, 146-152.
- [2] Intizar Ali, Abdul Hameed Memon, M. Tarique Bhatti, Dileep Kumar, Ishfaq Ali Qazi, Sajjad Banghwar, (2018) "Dynamic Fluid-Structure Interaction Analysis of Propeller Aircraft Wing. American Scientific Research Journal for Engineering, Technology, and Sciences, Volume 45, 64-74.
- [3] Faris Ahmed Mohammed Al-hadi, Mosab Adel Mohammed Ahmed, (2016) "Fluid Structure Interaction for Light Aircraft Wing (SAFAT 03)". Department of Aeronautical Engineering, Sudan University of Science and Technology.
- [4] Dario Aresta, (2017) "Aeroelastic Effects of a Very Flexible Transonic Wing: Fluid-Structure Interaction Study". Department of Aerospace Engineering, Técnico Lisboa. 1-74.
- [5] A Arun Kumar, N Manoj, Amit Kumar Onkar, M Manjuprasad, (2015) "Fluid-Structure Interaction analysis of a Cropped Delta Wing". 12th International Conference on Vibration Problems, ICOVP, 1205-1212.
- [6] Rabii El Maani, Bouchaib Radi and Abdelkhalak El Hami, (2017) "Vibratory Reliability Analysis of an Aircrafts Wing via Fluid-Structure Interactions". Journal, Aerospace, 2-16.
- [7] A Ramesh Kumar, S.R Balakrishnan and S Balaji, "Design of and Aircraft Wing structure for Static Analysis and Fatigue Life Prediction". Department of Aeronautical Engineering, Nehru institute of engineering and technology.



10.22214/IJRASET



45.98



IMPACT FACTOR:
7.129



IMPACT FACTOR:
7.429



INTERNATIONAL JOURNAL FOR RESEARCH

IN APPLIED SCIENCE & ENGINEERING TECHNOLOGY

Call : 08813907089  (24*7 Support on Whatsapp)